

A theoretical analysis of formation flight as a nonlinear self-organizing phenomenon

TAKESHI SUGIMOTO

Faculty of Engineering, Kanagawa University, 3-27-1 Rokkakubashi, Kanagawa Ward, Yokohama, 221-8686, Japan

[Received on 29 October 2001; revised on 20 June 2002]

This study analyses the existence, stability and self-organization of formation flight utilized by migrant birds. Air is approximated as an incompressible inviscid flow, while birds are modelled as elliptically loaded lifting-lines. Application of conventional wing theory leads to newly derived, basic equations that describe the problem as a dynamical system of multiple wings interacting with each other through induced flow field. Formation flight is defined as the steady-state solution of the basic equations, in particular the solution that all the birds fly at the same speed. In the case of a prescribed thrust, constant transverse interval between adjacent birds, and a flock of physically identical birds, analytical study of the basic equations reveals the facts that (1) formation flight is self-organized and (2) this formation flight is stable. The new implication is that a configuration of formation emerges as a result of nonlinear dynamical interaction between many birds and that this nonlinear dynamical system does not exhibit chaotic behaviour. Numerical calculation has also been done for cormorant-type birds with the same transverse interval between flock members. The proposed numerical scheme quickly converges to very accurate results owing to the recently derived, closed-form expression of induced velocity distribution around an elliptically loaded lifting-line. Transverse intervals between birds are found to be a more important factor than the number of birds. Configurations of formations are found to be inverted U rather than inverted V. In these formations every bird enjoys the same amount of drag reduction.

Keywords: dynamical system; formation flight; lifting line theory; self-organization.

1. Introduction

Large water birds are often observed to fly in a formation. As Ohanian (1998) recently wondered,

Strings of migrating geese and ducks (and also fleets of bombers) usually fly in a V-formation. Is there a physical reason for this? Presumably the wingtip of each goose generates a trailing vortex, as the air spills around the wing tip from the high-pressure zone above. Is the following goose trying to gain extra lift from the upward flow in this vortex? If so, the leading goose has the hardest job. Do the geese take turns at leading?

The effect of drag reduction in formation flight was noted at the dawn of aeronautics, so let us recall the major former efforts to understand the physics of formation flight.

In 1914, one year after Prandtl published his lifting-line theory, his collaborator Wieselsberger pointed out the possibility that induced drag could be reduced owing to the velocity field induced by bound and trailing vortices of nearby flock members (Wieselsberger, 1914). He replaced a bird by a horseshoe vortex with constant strength, and considered three birds in a staggered formation, i.e. a diagonal-line formation. His sample calculation showed the bird in the middle gains 15.8% drag saving, but he did not give an explanation of the V formation.

In the early 1940s Schlichting (1942, 1944) published two papers related to formation flight. His first paper (Schlichting, 1942) analysed interaction among multiple airplanes by using horseshoe vortices and prescribing V, transverse-line, and inverted-V formations. He calculated rates of energy savings for various aircraft numbers, and recommended inverted-V formations for practical reasons, i.e. visibility and almost evenly distributed drag. His second paper (Schlichting, 1944) treated how variation in altitude affects power savings in formation flight and reached the conclusion that vertical staggering did not bring any advantages to power savings.

Lissaman & Shollenberger (1970) studied flight formation. They calculated and showed drag saving in terms of bird spacing and the number of flock members. They also showed a sample configuration of flight formation with the constraint that induced drag be the same for all flock members, that is a parabola-like, inverted U. Their argument relies on lifting-line theory, too. They tried an intuitive explanation of stability: if a bird A speeds up and flies ahead of the formation, then this reduces its beneficial interference with its neighbours and results in increase in the bird A's drag; thus the bird A may be pulled back into the formation. This scenario is not trivial because the phenomenon is governed by nonlinear interaction between many birds. This paper tests their conjecture in a mathematically rigorous manner.

Since the 1970s, Hummel has been studying formation flight as an energy-saving mechanism, for application to air carriers. He extended Schlichting's horse-shoe vortex method to analyse formation flight among wings with different spans (Hummel, 1973, 1978). His calculation showed energy-saving effects by prescribing a diagonal-line, V, inverted-V, and other configurations among birds with the same or different sizes. The inverted-U formation was also found for nearly uniform drag condition. Asymmetry of velocity fields in a formation introduces yaw and roll to individuals. Hummel investigated this effect and found it negligible (Hummel & Bock, 1981). His findings were summarized (Hummel, 1983). He also conducted experiments using two aircraft (Beukenberg & Hummel, 1986). In the experiments he confirmed an energy-saving effect. To analyse the two-aircraft situation he also applied lifting surface theory and found little discrepancy between horse-shoe vortex and lifting surface analyses (Hummel & Beukenberg, 1989). All his findings are summarized in the recent literature (Hummel, 1995, 1996).

Filippone (1996) described bird formation flight by use of a horse-shoe vortex method. By giving *a priori* geometry of formations, he calculated induced drag distribution over a flock. He also used various heuristic optimization techniques to solve nonlinear equations to determine the configuration that ensures that every bird has the same amount of induced drag. He, too, found a parabola-like, inverted-U formation.

In 2001 biologists obtained evidence of energy saving in V-formation flight using direct measurements of well-trained pelicans (Weimerskirch *et al.*, 2001). Their measurements show the facts: the rate of wing beat in the most advantageous position in a formation goes

down to as low as 45% of a solo flight case; the rate of heart beat in a formation also goes down to 8/9 that of solo flight. As Rayner (2001) points out, the evidence confirms the aerodynamic prediction. Of course, as we shall discuss later, formation flight has aerodynamic as well as behavioural aspects, but it should be emphasized that the former aspect has been established.

Within this historical context we aim at an understanding of the nonlinear dynamics of formation flight, for many of the former studies have focused on energy-saving effects and the shapes of formations in a steady state.

To accomplish our aim we have tried to make our analysis not only as mathematically rigorous as possible but also as numerically accurate as possible. As a consequence, this becomes the second feature of the present study.

Another important feature is the use of the recently derived formula for induced flow of an elliptic lifting-line system (Sugimoto, 2002). Most of the former studies made use of horse-shoe vortices to analyse interaction among birds or aircraft. However, we know that the conservation of fluid energy is violated by replacing a sheet of wake vorticity with a pair of vortex filaments. As Lighthill (1989, p. 219) describes,

Finally, it rolls up into a pair of *relatively* narrow line vortices, . . .

As is already known, these *relatively* (Lighthill's italic) narrow vortices are quite well modelled by circular vortices (Milne-Thomson, 1973). The radius of these circular vortices is 0.219 times semi-span, and 10.4% of the total fluid energy is confined within these vortices. The work done by drag exactly balances the total energy within the fluid in the plane perpendicular to the wake. To replace a vortex sheet by a pair of line vortices is equivalent to ignoring the 10% energy conveyed by wake vorticity. Therefore, our study deals with the full lifting-line system: the vorticity bounded upon wings and flat sheets of their wake. The flat-wake model may not be very realistic. However, it does not violate the conservation of fluid energy and it is simple enough to allow analytic treatments. By this model we derive the formula to extend the former studies and make our analysis sound within the realm of the physical model to be used.

This paper is organized as follows. Section 2 describes vortex dynamics for our model and basic equations. To describe the flow field we make use of the closed-form formula for induced flow around an elliptically loaded wing in the $z = 0$ plane. Section 3 presents an analysis and discussion on the nature of flow field around a lifting-line system and the existence and stability of stationary solutions of the basic equations: all the former studies treated stationary solutions only. Section 4 shows numerical results for cormorants in a formation. The recently derived formula for induced flow plays an important role. Firstly, owing to this, one can introduce a semi-analytical method of solution and obtain very accurate results with seven significant digits. Secondly, the formula can afford much information of the flow field around a wing, and this aids the understanding of the physics behind the self-organization of formations. Studies are conducted on effects due to the transverse intervals between birds and the number of birds. Sample calculation shows inverted-U configurations again. Annotation of the results leads to discussion on the physical and social nature of flight formations. Section 5 summarizes the findings.

2. Theory

2.1 Assumptions

In this study all quantities are measured in mks units.

As flight speed is low and Reynolds number is high, it is appropriate to treat air as an inviscid and incompressible fluid. Following conventional wing theory, however, we shall model the very basic effects of viscosity by so-called zero-lift drag.

Vorticity distributes over a body surface and in wake. Vorticity over the body surface is called bound vorticity, which is the main source of aerodynamic forces. Lifting-line theory approximates bound vorticity by a single filament having vorticity distribution. This theory is well known to predict the velocity field around a high aspect ratio wing as well as induced drag, which is brought about in return for lift generation. Larger birds are known to make the most of formation flight, and their aspect ratio is at least larger than ten. Therefore it is appropriate to adopt lifting-line theory for this study.

In steady states a trailing vortex sheet consists of a streamwise vorticity in the wake. But due to non-steady motion, transverse components of vorticity will be shed into the wake. This study neglects effects due to the transverse vorticity in the wake for the following reasons: (1) acceleration or deceleration of bird flight is as moderate as quasi-steady motion; (2) periodic shedding of positive and negative vorticity by wing flapping is cancelled out in a time-averaged sense. Larger birds are known to flap wings slowly and manoeuvre slowly. Unsteadiness in lifting-line theory is well classified by typical length scales and wave length due to unsteady motion (Wilmott, 1988). Let c_{\max} , s , U , and f denote the maximum chord, full-span, flight velocity, and the frequency of the motion, then the relation

$$c_{\max} \ll s/2 \ll U/f$$

holds for the slow flapping flight of large birds. For example (Tennekes, 1996), if a cormorant, with a semi-span of 0.8 m and a root chord of 0.2 m, flies at the cruising speed of 15 m s^{-1} by flapping its wing one or two times a second, then the wavelength U/f becomes around $7.5 \approx 15 \text{ m}$, which is 10–20 times larger than the semi-span. This frequency regime is called Regime I, in which a quasi-steady theory is adequate and unsteady effects are of smaller order than three-dimensional effects (Wilmott, 1988). The most powerful support for this assumption is the fact that direct measurements showed the reduction of wing beat in a formation as reported by Weimerrskirch *et al.* (2001). The quasi-steady theory takes account of apparent mass effect along with steady aerodynamics.

Thus the steady lifting-line theory is a fairly good approximation to study the skeletal structure of the physics behind formation flight.

Forces acting on a bird are given by the following volume integral (Lighthill, 1989; Saffman, 1992):

$$\mathbf{F} = \rho \int \mathbf{u} \times \boldsymbol{\omega} dV, \quad (2.1)$$

where \mathbf{F} , ρ , \mathbf{u} , and $\boldsymbol{\omega}$ denote an aerodynamic force vector, air density, a velocity vector, and a vorticity vector, respectively. The velocity vector and the vorticity vector are interrelated by

$$\boldsymbol{\omega} = \nabla \times \mathbf{u}. \quad (2.2)$$

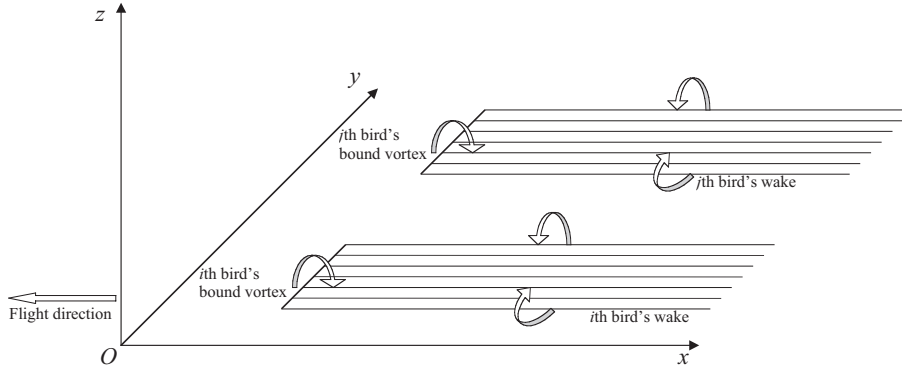


FIG. 1. Coordinate system and vortex systems. Thick lines denote bound vortices, and thin lines represent wake vorticity. Curved arrows indicate typical directions of vortex rotation, when positive lift is generated. The coordinate system x and y are non-dimensionalized by use of the root chord c_{max} and the semi-span $s/2$, respectively.

Velocity field consists of two components. One is uniform flow relative to the bird, corresponding to its forward flight. Another is velocity induced by distributed vorticity. When vorticity distribution is known, Biot–Savart’s relation, an inverted version of (2.2), gives induced velocity \mathbf{u} :

$$\mathbf{u}(\mathbf{r}) = \frac{1}{4\pi} \int \frac{\boldsymbol{\omega}(\mathbf{r}') \times (\mathbf{r} - \mathbf{r}')}{|\mathbf{r} - \mathbf{r}'|^3} dV(\mathbf{r}'), \quad (2.3)$$

where \mathbf{r} and \mathbf{r}' denote the position vectors of \mathbf{u} and $\boldsymbol{\omega}$, respectively.

Throughout this study I shall use x and y coordinates non-dimensionalized by use of the root chord c_{max} and the semi-span $s/2$, respectively.

Figure 1 shows the coordinate system and the vortex systems that stand for birds in a flock. We take x and y coordinates following aeronautical convention as shown in Fig. 1, but z should be a relative altitude. Every bird, with its bound vortex parallel to the y direction, is assumed to fly toward the negative- x direction at the same altitude, $z = 0$. The reason for the proposed layout, where every bird flies at the same altitude, is given as follows. The i th bird’s drag, a force parallel to the flight direction, is affected most strongly by the neighbouring j th bird, if a z -component of velocity induced by the j th bird becomes the largest. The equation (2.3) shows this occurs if both i th and j th birds are at the same altitude for the fixed x and y components.

The situation depicted in Fig. 1 and (2.1) leads to the fact that there is no transverse force to change y -directional intervals between birds, because there is no y -directional component in induced velocity nor z -directional component of the vorticity. Thus the transverse intervals remain unchanged in the present problem and so this study treats transverse intervals as given quantities.

It is also pointed out that, in the wake, velocity vectors are parallel to the wake vorticity, and hence the wake will not generate forces.

The study does not consider the aerodynamic moments, because their effects are known to be of negligible order (Hummel & Bock, 1981).

2.2 Derivation of basic equations

The lift acting on the i th bird is expressed as

$$\rho \int_{\text{wing}} u_i \omega_i dV = \frac{1}{2} \rho u_i^2 S_i C_{L_i}, \quad (2.4)$$

where the subscript i is used to identify i th bird quantities; u_i , ω_i , S_i , and C_{L_i} designate horizontal velocity, bound vorticity, wing area and lift coefficient, respectively. The left-hand side of (2.4) is a lift component of (2.1), while the right-hand side is an expression of lift after conventional wing theory. It should be noted that the identity (2.4) leads to the relation that ω_i is in proportion to $u_i C_{L_i}$, and hence velocity due to this vorticity is also in proportion to $u_i C_{L_i}$. Using these relations one can estimate induced drag as

$$-\rho \int_{\text{wing}} (\text{velocity}) \omega_i dV \propto \begin{cases} \rho u_i^2 C_{L_i}^2 & \text{for self-induction} \\ \rho u_i u_j C_{L_i} C_{L_j} & \text{for interaction with } j\text{th bird.} \end{cases} \quad (2.5)$$

Introducing interaction functions G_{ji} , the j th bird's influence upon the i th bird, induced drag can be written as

$$\sum_{j=1}^n \left\{ \frac{1}{2} \rho u_i u_j S_i C_{L_i} C_{L_j} \frac{G_{ji}}{\pi \mathcal{R}_j} \right\},$$

where the factor $\pi \mathcal{R}_j$ is introduced to normalize the self-interaction; \mathcal{R}_j denotes the aspect ratio of the j th bird's wing; n is the total number of birds. An interaction function is given by the normalized integral of a product of induced velocity and vorticity distribution. An explicit form for an elliptically loaded wing is given in Section 3.

Let us derive equations of motion for the i th bird. As described in the assumptions, altitude is desired to be constant. This means that a vertical equilibrium must always be fulfilled:

$$m_i g = \frac{1}{2} \rho u_i^2 S_i C_{L_i}, \quad (2.6)$$

where m_i and g denote the i th bird's mass and the acceleration due to gravity, respectively.

On the other hand, the equation for horizontal motion is given by

$$m_i \dot{u}_i = \frac{1}{2} \rho u_i^2 S_i C_{D0_i} + \sum_{j=1}^n \left\{ \frac{1}{2} \rho u_i u_j S_i C_{L_i} C_{L_j} \frac{G_{ji}}{\pi \mathcal{R}_j} \right\} - T_i, \quad (2.7)$$

where a single dot denotes the first derivative with respect to time; the first and second terms on the right-hand side are zero-lift drag and induced drag, respectively; the third term is i th bird's thrust.

Solving (2.6) with respect to C_{L_i} and substituting this relation for (2.7), some algebra leads to

$$\dot{u}_i = \alpha_i u_i^2 + \sum_{j=1}^n \beta_j G_{ji} u_i^{-1} u_j^{-1} - \tau_i, \quad (2.8)$$

where

$$\alpha_i = \frac{\rho S_i C_{D0i}}{2m_i},$$

$$\beta_j = \frac{2m_j g^2}{\pi \mathcal{R}_j \rho S_j},$$

and

$$\tau_i = \frac{T_i}{m_i},$$

Both α_i and β_j are given positive constants.

Since our aim is to consider how the dynamics of formation flight behaves intrinsically, or without controlling anything, the thrust is assumed to be a given value, consisting of positive average thrust and sinusoidal fluctuation:

$$\tau_i = \bar{\tau}_i + \delta\tau_i \exp i\Omega t,$$

where

$$\bar{\tau}_i = \lim_{t \rightarrow \infty} \frac{1}{t} \int_0^t \tau_i dt;$$

$\delta\tau_i$ and Ω denote the amplitude and circular frequency of fluctuation, respectively. The constant thrust is also an optimum strategy for long-distance flight, which is discussed briefly in the Appendix.

A set of (2.8) for $i = 1, 2, \dots, n$ governs the mechanics of formation flight. The dynamics can be represented by u_i , and the geometry of formation by G_{ji} .

We shall examine the existence and stability of the stationary solutions of (2.8). What we call formation flight is the stationary solution of (2.8), such that every birds flies at the same velocity.

3. Analytical results and discussion

This section clarifies the necessary condition for the feasibility of formation flight to a general extent and the global and asymptotic stability of formations for a particular case by using the nature of the flow field about a flock.

3.1 Nature of induced velocity distribution around an elliptic lifting-line system

To study the mechanics of formation flight, it is necessary to know the induced velocity field around a wing. As stated in the previous section, this study is interested in the z -component of velocity induced by another bird at the same altitude, i.e. $z = 0$. We denote this velocity component, in short induced velocity, by $w(x, y, 0)$ or simply $w(x, y)$.

Most former studies made use of a horse-shoe vortex with constant strength, but this study assumes a vortex system with an elliptic load distribution. An elliptic load

distribution possesses favourable features: (1) it is more realistic than uniform load distribution; (2) it corresponds to the first harmonics of Fourier series and (3) it is known to induce minimum drag upon a single wing, and hence subtle effects due to formation flight can be examined. A wing is placed upon a segment $[-1, 1]$ of the y -axis. The vortices bounded upon the wing are given by using the circulation $\gamma(y)$

$$\begin{aligned}\omega &= (0, \gamma(y), 0) \\ &= \left(0, \frac{\epsilon u \gamma_0}{2} \sqrt{1 - y^2}, 0\right) \text{ for } y \in [-1, 1],\end{aligned}\quad (3.1)$$

where ϵ , u and γ_0 designate the ratio of root chord to semi-span, flight velocity and the circulation at the wing root, respectively.

The wake consists of changes in the vorticity shed from the wing:

$$\begin{aligned}\omega &= \left(-\frac{d\gamma(y)}{dy}, 0, 0\right) \\ &= \left(-\frac{\epsilon u \gamma_0}{2} \frac{d}{dy} \left\{\sqrt{1 - y^2}\right\}, 0, 0\right) \text{ for } x \times y \in [0, \infty) \times [-1, 1].\end{aligned}\quad (3.2)$$

Until recently it was not known whether there existed a closed-form expression for induced velocity distribution around an elliptically loaded wing in the $z = 0$ plane: its derivation seemed awkward (see Phillips, 1985 for the known analytic formulae). But it is not as cumbersome as might be thought (Sugimoto, 2002). Let us start by substituting the vorticity distribution (3.1), (3.2) for (2.3). The following integral calculates velocity induced at a field point (x, y) by these vortices:

$$\begin{aligned}w(x, y) &= \frac{\epsilon \gamma_0}{8\pi} \int_{-1}^1 \frac{-\epsilon x \sqrt{1 - \eta^2}}{\{\epsilon^2 x^2 - (y - \eta)^2\}^{3/2}} d\eta \\ &\quad - \frac{\epsilon \gamma_0}{8\pi} \int_{-1}^1 \int_0^\infty \frac{y - \eta}{\{(\epsilon x - \xi)^2 - (y - \eta)^2\}^{3/2}} \frac{d}{d\eta} \left\{\sqrt{1 - \eta^2}\right\} d\xi d\eta.\end{aligned}$$

Integrating the second term on the right-hand side of the equation above in terms of ξ , one obtains the induced velocity in a non-dimensional, more concise form, g :

$$\begin{aligned}g(x, y) &= \frac{8\pi}{\epsilon \gamma_0} w(x, y) \\ &= \int_{-1}^1 \sqrt{1 - \eta^2} \left\{1 + \frac{\epsilon x}{\sqrt{\epsilon^2 x^2 + (y - \eta)^2}}\right\} \frac{d\eta}{(y - \eta)^2},\end{aligned}\quad (3.3)$$

where we take Hadamard's finite part of the improper integral above.

The function G_{ji} , which governs the aerodynamic interaction between birds, is given by substituting the induced velocity distribution (3.3) for (2.1):

$$G_{ji} = -\frac{2}{\pi^2} \int_{-1}^1 \sqrt{1 - \eta^2} g(x_{ji}, Y_{ji}) d\eta, \quad (3.4)$$

where Y_{ji} designates $\eta + |y_{ji}|$; x_{ji} and y_{ji} are respectively the x and y components of the distance between the j th and i th birds and g is $-\pi$ for $j = i$, while g for $j \neq i$ is given by a positive-valued function

$$\begin{aligned}
 g(x_{ji}, Y_{ji}) = & \pi \frac{Y_{ji} - \sqrt{Y_{ji}^2 - 1}}{\sqrt{Y_{ji}^2 - 1}} \\
 & + \frac{2\epsilon_j x_{ji}}{\left[\left\{ \epsilon_j^2 x_{ji}^2 + (Y_{ji} - 1)^2 \right\} \left\{ \epsilon_j^2 x_{ji}^2 + (Y_{ji} + 1)^2 \right\} \right]^{1/4}} \\
 & \times \left\{ \frac{Y_{ji}}{Y_{ji} - \sigma_{ji}} \mathbf{II}(n_{ji}, k_{ji}^2) + \frac{\sigma_{ji} Y_{ji}}{1 - \sigma_{ji} Y_{ji}} \mathbf{K}(k_{ji}^2) \right. \\
 & \left. - \frac{(1 - \sigma_{ji}^2) Y_{ji}}{(1 - \sigma_{ji} Y_{ji})(Y_{ji} - \sigma_{ji})} \mathbf{E}(k_{ji}^2) \right\} \tag{3.5}
 \end{aligned}$$

where

$$n_{ji} = \frac{1 - \sigma_{ji} Y_{ji}}{Y_{ji}(Y_{ji} - \sigma_{ji})},$$

$$k_{ji}^2 = \frac{\sigma_{ji}(1 - \sigma_{ji} Y_{ji})}{(1 - \sigma_{ji}^2) Y_{ji}},$$

$$\sigma_{ji} = \delta_{ji} - \sqrt{\delta_{ji}^2 - 1},$$

$$\delta_{ji} = \frac{\epsilon_j^2 x_{ji}^2 + Y_{ji}^2 + 1}{2Y_{ji}},$$

$$\epsilon_j = \frac{4}{\pi \mathcal{R}_j}.$$

Functions \mathbf{II} , \mathbf{K} , and \mathbf{E} in (3.5) are the complete elliptic integrals of three kinds. It should be emphasized that the use of (3.5) does not violate the conservation of energy.

Studying (3.3), (3.4), and (3.5), we are led to the following statements. Supposing that all the n birds, having elliptically loaded circulation, fly together at the same altitude, then

- (1) Any interaction function between one bird and another is always negative:

$$G_{ji} < 0 \quad \text{if } j \neq i; \tag{3.6}$$

It can be found in standard textbooks (Lighthill, 1989; Milne-Thomson, 1973) that the self-interaction function is always positive. That is

$$G_{ii} > 0.$$

- (2) The interaction functions are odd and monotonically decreasing in a streamwise direction in terms of $x_{ji} = x_i - x_j$, the x -component of the distance from the j th bird's centre of bound vortex to that of the i th bird:

$$\partial_x G_{ji} < 0, \quad (3.7)$$

where

$$\partial_x G_{ji} = \frac{\partial G_{ji}}{\partial x_{ji}}.$$

- (3) The first derivative of interaction functions with respect to x_{ji} are even functions of x_{ji} :

$$(\partial_x G_{ji})_{x_{ji}=-x} = (\partial_x G_{ji})_{x_{ji}=x}. \quad (3.8)$$

In reality the above-mentioned statements hold true for formation flight of n birds having *non-negative* circulation.

3.2 Global attractiveness and feasibility of formation flight

This section examines the feasibility of formation flight on the basis of (2.8). We shall make the most of the phase portrait, because it depicts behaviours of formation flight, and upper and lower bounds for acceleration help us confirm the existence of a global attractor to (2.8).

An upper bound for the right-hand side of (2.8) can be obtained by dropping all the interaction terms and using the minimum thrust:

$$\alpha_i u_i^2 + \beta_i G_{ii} u_i^{-2} - \bar{\tau}_i + \delta\tau_i, \quad (3.9)$$

because interaction terms are negative. It should be noted that the upper bound corresponds to the solo flight condition. Let us define two critical velocities by equating the expression above with zero:

$$u_{iTO} = -\sqrt{\frac{\bar{\tau}_i - \delta\tau_i - \sqrt{(\bar{\tau}_i - \delta\tau_i)^2 - 4\alpha_i\beta_i G_{ii}}}{2\alpha_i}}, \quad (3.10)$$

and

$$u_{iF+} = -\sqrt{\frac{\bar{\tau}_i - \delta\tau_i + \sqrt{(\bar{\tau}_i - \delta\tau_i)^2 - 4\alpha_i\beta_i G_{ii}}}{2\alpha_i}}. \quad (3.11)$$

Then the upper bound (3.9) becomes negative for $u_i \in (u_{iF+}, u_{iTO})$ and non-negative otherwise. Critical velocities u_{iF+} and u_{iTO} roughly correspond to the cruising and take-off velocities of solo flight, respectively.

Let us proceed to the estimation of lower bounds. The inequalities (3.6) and (3.7) assure

$$\begin{cases} G_{ii} > 0, \\ 0 > G_{ji} > G_{ji}^\infty \quad \text{for } j \neq i, \end{cases} \quad (3.12)$$

where

$$G_{ji}^{\infty} = \lim_{x_{ji} \rightarrow \infty} G_{ji}.$$

This study confines its discussion on birds' flight to the following case:

$$u_{jTO} \geq u_j \text{ for all } j. \quad (3.13)$$

The relation above is equivalent to the condition that all the birds fly at velocities faster than take-off speeds. Formation will be made in the air after every bird takes off. So the inequality (3.13) holds.

Relations (3.12) and (3.13) lead to

$$0 > \beta_j G_{ji} u_j^{-1} u_i^{-1} > \beta_j G_{ji}^{\infty} u_{jTO}^{-1} u_i^{-1}.$$

The rightmost expression consists of a lower bound. Using the relation above, one finds the lower and upper bounds for the right-hand side of (2.8):

$$\begin{aligned} \alpha_i u_i^2 + \beta_i G_{ii} u_i^{-2} - \bar{\tau}_i + \delta\tau_i &> \alpha_i u_i^2 + \sum_{j=1}^n \beta_j G_{ji} u_i^{-1} u_j^{-1} - \tau_i \\ &> \alpha_i u_i^2 + \beta_i G_{ii} u_i^{-2} - \bar{\tau}_i - \delta\tau_i + \left\{ \sum_{j \neq i} \beta_j G_{ji}^{\infty} u_{jTO}^{-1} \right\} u_i^{-1}. \end{aligned} \quad (3.14)$$

The last term of the lower bound is a hyperbola in terms of u_i , and its coefficient in braces is a positive constant.

One can derive a tighter lower bound if

$$u_{jF+} \geq u_j \text{ for all } j.$$

Replacing u_{jTO} with u_{jF+} , one obtains another lower bound:

$$\alpha_i u_i^2 + \beta_i G_{ii} u_i^{-2} - \bar{\tau}_i - \delta\tau_i + \left\{ \sum_{j \neq i} \beta_j G_{ji}^{\infty} u_{jF+}^{-1} \right\} u_i^{-1}. \quad (3.15)$$

The acceleration \dot{u}_i is a single-valued explicit function with respect to u_i , and hence the i th bird's phase portrait of formation flight must be located somewhere in between these bounds. Figure 2 shows a sample locus of the i th bird's flight as a solid line meandering in a region between the upper and lower bounds. In this figure the lower bounds #1 and #2 denote those in (3.14) and (3.15), respectively. Another critical velocity u_{iF-} shown in Fig. 2 is defined as the intersection between the u_i -axis and the lower bound #2:

$$u_{iF-} = -\frac{1}{2} \left\{ \sqrt{p+v} + \sqrt{p-v + \frac{2q}{\sqrt{p+v}}} \right\}, \quad (3.16)$$

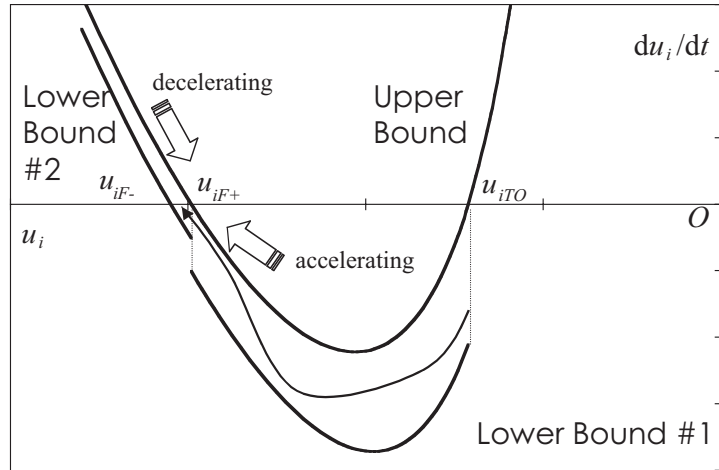


FIG. 2. Typical phase portrait of i th bird's flight in a formation. The upper bound is given by (3.9) and the lower bounds #1 and #2 denote (3.14) and (3.15), respectively.

where

$$v = \frac{a - bc}{1 - c},$$

$$a = \frac{32pr + 9q^2}{24pr + 2p^2}(-1 + d),$$

$$b = \frac{32pr + 9q^2}{24pr + 2p^2}(-1 - d),$$

$$c = \left\{ 1 + \frac{96pr + 27q^2}{72pr + 27q^2 - 2p^3}d \right\}^{-1/3},$$

$$d = \sqrt{1 - 4 \frac{(12r + p^2)(16r^2 + 12p^2r + 3pq^2)}{(32pr + 9q^2)^2}},$$

$$p = \frac{\bar{\tau}_i + \delta\tau_i}{\alpha_i},$$

$$q = \frac{\sum_{j \neq i} \beta_j G_{ji}^\infty u_{jF+}^{-1}}{\alpha_i},$$

$$r = \frac{\beta_j G_{ii}}{\alpha_i}.$$

Let us consider the global attractiveness of the state where $\dot{u}_i = 0$ and $u_i \in (u_{iF-}, u_{iF+})$. To annotate the phase portrait one should recall the present notation: (1) a bird is flying toward the negative x -direction; (2) therefore u_i is negative; (3) the upper and lower halves about the u_i -axis correspond to deceleration and acceleration regions, respectively.

Firstly let us think about the meaning of u_{iTO} as the velocity limit of stable take-off. Suppose a flight condition of a bird goes along the upper bound: (1) the bird will be decelerated, if it flies slower than u_{iTO} ; (2) the bird will be accelerated otherwise. This leads to a necessary condition for stable take-off: fly faster than u_{iTO} .

Once a bird takes off at a velocity faster than u_{iTO} , then this bird will be accelerated toward the condition, that is $\dot{u}_i = 0$ and $u_i \in (u_{iF-}, u_{iF+})$. Even if the flight condition goes further into the region $\dot{u}_i > 0$, then the bird is decelerated. Thus the flight condition, $\dot{u}_i = 0$ and $u_i \in (u_{iF-}, u_{iF+})$, globally attracts any motion of a bird. Henceforth we call this flight condition the cruising state.

If we take a look at (3.14), then it becomes clear that the basic mechanism is well described by the equation of solo flight with the minimum thrust:

$$\dot{u}_i = \alpha_i u_i^2 + \beta_i G_{ii} u_i^{-2} - \bar{\tau}_i + \delta \tau_i. \quad (3.17)$$

This can be solved analytically, but implicitly,

$$\left(\frac{u_i - u_{iF+}}{u_i + u_{iF+}} \right)^{-u_{iF+}} \left(\frac{u_i + u_{iTO}}{u_i - u_{iTO}} \right)^{-u_{iTO}} = \kappa \exp \left[-2\alpha_i \left(u_{iF+}^2 - u_{iTO}^2 \right) t \right], \quad (3.18)$$

where κ is an arbitrary constant depending on the initial value. There is a stable steady-state solution at $u_i = u_{iF+}$, and Fig. 3 shows a sample of time history. Initially a bird is exponentially accelerated; meanwhile the velocity becomes almost proportional to time; in the end the motion is exponentially attracted to the steady state, i.e. $\dot{u}_i = 0$ and $u_i = u_{iF+}$. The following relation holds at the equilibrium:

$$\left(\frac{\partial \dot{u}_i}{\partial u_i} \right)_{u_i=u_{iF+}} < 0,$$

that is

$$G_{ii} < \frac{\alpha_i u_{iF+}^4}{\beta_i}. \quad (3.19)$$

This inequality assures the existence of restoring forces toward the equilibrium and hence the necessary condition of its stability.

Thus the cruising state, $\dot{u}_i = 0$ and $u_i \in (u_{iF-}, u_{iF+})$, plays a vital role as a global attractor even in formation flight. That is, formation flight is feasible only at this cruising state. On the other hand, formation flight means that every flock member flies at the same velocity. Therefore, the following statement becomes a necessary condition for the

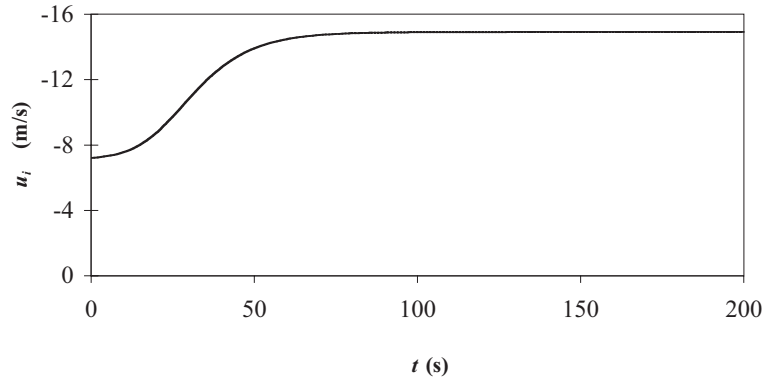


FIG. 3. Typical time history of solo flight. The sample calculation is given by (3.18) using the data in Section 4.1.

feasibility of formation flight:

$$\bigcap_{i=1}^n (u_{iF-}, u_{iF+}) \neq \emptyset, \quad (3.20)$$

that is, every flock member has a possible range of the cruising state overlapping all the other members'.

It should, however, be noted that the feasibility requirement (3.20) does not ensure the existence or uniqueness of formation flight.

3.3 Existence of formation flight

The previous section showed the necessary condition for the feasibility of formation flight in a rather general sense. In this section a proof is given of the existence of flight formation for physically identical birds flying with constant thrust at a transverse interval.

We shall treat the case that every flock member has the same parameters:

$$\forall \alpha_i = \alpha, \quad \forall \beta_i = \beta, \quad \forall \bar{\tau}_i = \bar{\tau}, \quad \forall \delta\tau_i = \delta\tau.$$

Then one obtains relations on velocities and the equations of motion without $\delta\tau$ terms:

$$\begin{aligned} \dot{x}_i &= c_{\max}^{-1} u_i, \\ \dot{u}_i &= \alpha u_i^2 + \beta \sum_{j=1}^n G_{ji} u_i^{-1} u_j^{-1} - \bar{\tau}, \quad \text{for } i = 1, 2, \dots, n \end{aligned} \quad (3.21)$$

where x_i designates the x -coordinate of the i th bird. The flock members are given numbers ranging from number one upon the far left to n upon the far right. In this case the necessary condition (3.20) is fulfilled, because all the possible ranges of flock members' cruising speeds coincide with one another's'.

If formation flight or an equilibrium exists, then the following must hold:

$$\begin{aligned} \dot{x}_i &= c_{\max}^{-1} \bar{u}, \\ 0 &= \alpha \bar{u}^2 + \beta \sum_{j=1}^n \bar{G}_{ji} \bar{u}^{-2} - \bar{\tau}, \quad \text{for } i = 1, 2, \dots, n \end{aligned} \tag{3.22}$$

where \bar{u} denotes the terminal velocity of an entire flock given by

$$\bar{u} = -\sqrt{\frac{\bar{\tau} + \sqrt{\bar{\tau}^2 - 4\alpha\beta \sum_{j=1}^n \bar{G}_{ji}}}{2\alpha}}; \tag{3.23}$$

\bar{G}_{ji} denotes the interaction function in a steady formation and is a function of unknown $x_{ji} = x_i - x_j$.

There are n different expressions of \bar{u} . Equating these, we obtain a set of $n - 1$ equations, which are reduced to

$$\sum_{j=1}^n \bar{G}_{j1} = \sum_{j=1}^n \bar{G}_{j2} = \dots = \sum_{j=1}^n \bar{G}_{jn}. \tag{3.24}$$

These equations determine a configuration of a flight formation, and we shall prove the existence of a solution set to (3.24). To complete the proof, it is convenient to use a conservation law in terms of interaction functions:

$$\sum_{i=1}^n \sum_{j=1}^n \bar{G}_{ji} = nG(n), \tag{3.25}$$

or

$$G(n) = \frac{1}{n} \sum_{i=1}^n \sum_{j=1}^n \bar{G}_{ji},$$

where $G(n)$ is an average of interaction functions and constant. The law insists that the total induced drag of the entire flock is conserved. This is not surprising because inviscid flow is conservative in its nature. One can verify the conservation law by differentiating the left-hand side of (3.25) by x_k

$$\begin{aligned} \sum_{i \neq k} \frac{\partial x_{ki}}{\partial x_k} \partial_x \bar{G}_{ki} + \sum_{j \neq k} \frac{\partial x_{jk}}{\partial x_k} \partial_x \bar{G}_{jk} &= -\sum_{i \neq k} \partial_x \bar{G}_{ki} + \sum_{j \neq k} \partial_x \bar{G}_{jk} \\ &= \sum_{i \neq k} \{ \partial_x \bar{G}_{ik} - \partial_x \bar{G}_{ki} \} \\ &= 0, \end{aligned} \tag{3.26}$$

because of the nature of flow field (3.8) and the identity of all the vortex systems. Relation (3.26) holds true for any x_k , so the left-hand side of (3.25) is found constant.

The advantage of formation flight can be seen through the average of interaction functions. We shall show that

$$G(n) < G(n-1). \quad (3.27)$$

Suppose the special situation of an n -bird formation: $n-1$ birds are flying closely together while one bird flies infinitely far downstream of all the other birds. Apparently $n-1$ upstream birds do not gain any upwash induced by the one flying far downstream. Therefore their portion of interaction functions is equivalent to the total of $n-1$ birds in a formation, i.e. $(n-1)G(n-1)$. The one far downstream enjoys the maximum merit from its flock members. Let the one far downstream be the i th bird and G_{ji}^∞ be this one's interaction function in terms of the j th bird. Using the inequality (3.12), it follows that

$$\sum_{j=1}^n G_{ji}^\infty < G(n). \quad (3.28)$$

The total value of the entire flock's interaction functions must be equal to $nG(n)$, so one reaches the inequality

$$\begin{aligned} nG(n) &= (n-1)G(n-1) + \sum_{j=1}^n G_{ji}^\infty \\ &< (n-1)G(n-1) + G(n), \end{aligned} \quad (3.29)$$

and hence (3.27) holds. The larger the flock becomes, the less induced drag acts on each flock member.

Now we shall show the existence of formation flight. The conservation law of interaction functions (3.25) can be rewritten as

$$(\mathbf{g}_n - G(n)\mathbf{e}_n^T) \cdot \mathbf{e}_n = 0, \quad (3.30)$$

where

$$\mathbf{g}_n = \left(\sum_{j=1}^n \bar{G}_{j1}, \sum_{j=1}^n \bar{G}_{j2}, \dots, \sum_{j=1}^n \bar{G}_{jn} \right),$$

$$\mathbf{e}_n = (1, 1, \dots, 1)^T.$$

The relation (3.30) implies that the locus of \mathbf{g}_n vector is confined upon the $(n-1)$ -dimensional hyperplane, perpendicular to \mathbf{e}_n , in n -dimensional space.

Now let us evaluate the value range that the sum of the i th bird's interaction functions can take. The largest value is $G(1)$ when this bird flies infinitely far upstream of all the other birds. The minimum value is attained when $n-1$ birds fly closely together infinitely upstream of the i th bird. In this case the total interaction functions of the i th bird can be given by $\sum_{j=1}^n G_{ji}^\infty$. Therefore the i th bird's total interaction functions can take values in between these bounds:

$$\sum_{j=1}^n G_{ji} \in \left[\sum_{j=1}^n G_{ji}^\infty, G(1) \right].$$

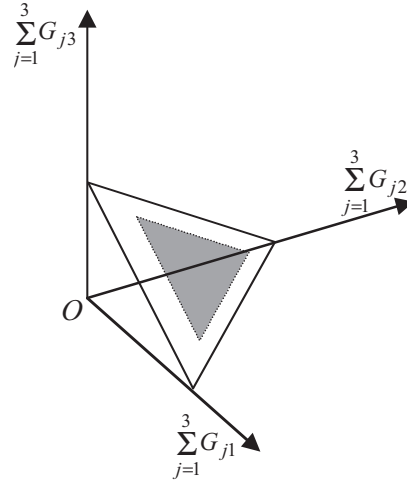


FIG. 4. Two-dimensional hyperplane representing the conservation law in three-dimensional space spanned by $(\sum_{j=1}^3 G_{j1}, \sum_{j=1}^3 G_{j2}, \sum_{j=1}^3 G_{j3})$. Shaded area corresponds to the feasible region.

The important thing is that interaction functions are continuous, and that the special value $G(n)$ is within this range. From (3.27) the following is obvious:

$$G(n) < G(1).$$

The relation above and the inequality (3.28) lead to

$$\sum_{j=1}^n G_{ji}^\infty < G(n) < G(1). \tag{3.31}$$

The derivation of this inequality is independent of the choice of the i th bird among the flock. The continuity of real-valued functions and the inequality (3.31) ensures the existence of a solution set to (3.24):

$$\sum_{j=1}^n G_{ji} = G(n) \text{ for all } i.$$

Figure 4 shows a hyperplane in the case of $n = 3$. The formation is fulfilled at the centre of the figure about this feasible region in the hyperplane.

3.4 Stability of formation flight

The study starts from the case of constant thrust, and then moves to the case of fluctuating thrust that simulates flapping. Let us study the linear stability of formation flight under small disturbances. Suppose the equilibrium is disturbed as

$$\begin{aligned} x_i &\rightarrow x_i + \delta x_i, \\ \bar{u} &\rightarrow \bar{u} + \delta u_i, \end{aligned}$$

then using (3.21) and (3.22) we are led to linearized equations on disturbances

$$\begin{aligned} \delta \dot{x}_i &= c_{\max}^{-1} \delta u_i, \\ \delta \dot{u}_i &\approx 2\alpha \bar{u} \delta u_i - \beta \bar{u}^{-3} \sum_{j=1}^n \bar{G}_{ji} (\delta u_i + \delta u_j) + \beta \bar{u}^{-2} \sum_{j=1}^n \partial_x \bar{G}_{ji} (\delta x_i - \delta x_j). \end{aligned} \quad (3.32)$$

Now we shall show that the following is a Liapunov function for the system (3.32):

$$H = \frac{1}{2} \sum_{i=1}^n (\delta u_i)^2 - \frac{c_{\max} \beta \bar{u}^{-2}}{4} \sum_{i=1}^n \sum_{j=1}^n \partial_x \bar{G}_{ji} (\delta x_i - \delta x_j)^2. \quad (3.33)$$

Firstly, the following relation holds:

$$H \geq 0, \quad (3.34)$$

because of the positiveness of the parameters, c_{\max} and β , and the inequality (3.7).

Let us take a first derivative of the function (3.33) with respect to time. Use of (3.22) and (3.32) leads to

$$\begin{aligned} \dot{H} &= \sum_{i=1}^n \delta u_i \delta \dot{u}_i - \frac{\beta \bar{u}^{-2}}{2} \sum_{i=1}^n \sum_{j=1}^n \partial_x \bar{G}_{ji} (\delta x_i - \delta x_j) (\delta u_i - \delta u_j) \\ &= 2\alpha \bar{u} \sum_{i=1}^n (\delta u_i)^2 - \beta \bar{u}^{-3} \sum_{i=1}^n \sum_{j=1}^n \bar{G}_{ji} (\delta u_i + \delta u_j) \delta u_i \\ &\quad + \beta \bar{u}^{-2} \sum_{i=1}^n \sum_{j=1}^n \partial_x \bar{G}_{ji} (\delta x_i - \delta x_j) \delta u_i - \frac{\beta \bar{u}^{-2}}{2} \sum_{i=1}^n \sum_{j=1}^n \partial_x \bar{G}_{ji} (\delta x_i - \delta x_j) (\delta u_i - \delta u_j). \end{aligned} \quad (3.35)$$

The last term on the right-hand side of (3.35) can be rewritten as

$$\begin{aligned} \sum_{i=1}^n \sum_{j=1}^n \partial_x \bar{G}_{ji} (\delta x_i - \delta x_j) (\delta u_i - \delta u_j) &= \sum_{i=1}^n \sum_{j=1}^n \partial_x \bar{G}_{ji} (\delta x_i - \delta x_j) \delta u_i \\ &\quad - \sum_{i=1}^n \sum_{j=1}^n \partial_x \bar{G}_{ji} (\delta x_i - \delta x_j) \delta u_j \\ &= 2 \sum_{i=1}^n \sum_{j=1}^n \partial_x \bar{G}_{ji} (\delta x_i - \delta x_j) \delta u_i, \end{aligned} \quad (3.36)$$

because

$$\partial_x \bar{G}_{ij} = \partial_x \bar{G}_{ji}.$$

The equality above is equivalent to (3.8), because every bird is the identical vortex system.

Substituting (3.36) for (3.35), one obtains a quadratic form in terms of velocity fluctuations as follows:

$$\begin{aligned}
\dot{H} &= 2\alpha\bar{u} \sum_{i=1}^n (\delta u_i)^2 - \beta\bar{u}^{-3} \sum_{i=1}^n \sum_{j=1}^n \bar{G}_{ji} (\delta u_i + \delta u_j) \delta u_i \\
&= \sum_{i=1}^n \left\{ 2\alpha\bar{u} - \beta\bar{u}^{-3} \sum_{j=1}^n \bar{G}_{ji} \right\} (\delta u_i)^2 - \beta\bar{u}^{-3} \sum_{i=1}^n \sum_{j=1}^n \bar{G}_{ji} \delta u_j \delta u_i \\
&= -\beta\bar{u}^{-3} \delta \mathbf{u}^T \mathbf{G} \delta \mathbf{u},
\end{aligned} \tag{3.37}$$

where

$$\delta \mathbf{u} = (\delta u_1, \delta u_2, \dots, \delta u_n)^T,$$

and

$$\mathbf{G} = \begin{pmatrix} G_{\Delta 0} & G_{\Delta 1} & G_{\Delta 2} & \cdots & G_{\Delta n-1} \\ G_{\Delta 1} & G_{\Delta 0} & G_{\Delta 1} & \cdots & G_{\Delta n-2} \\ G_{\Delta 2} & G_{\Delta 1} & G_{\Delta 0} & \cdots & G_{\Delta n-3} \\ \vdots & \vdots & \vdots & \ddots & \vdots \\ G_{\Delta n-1} & G_{\Delta n-2} & G_{\Delta n-3} & \cdots & G_{\Delta 0} \end{pmatrix}. \tag{3.38}$$

The diagonal component of the matrix above is given by

$$G_{\Delta 0} = \bar{G}_{ii} + \sum_{j=1}^n \bar{G}_{ji} - \frac{2\alpha\bar{u}^4}{\beta} < 0 \text{ for all } i. \tag{3.39}$$

The diagonal components are all the same because of (3.24). The inequality holds true for the following reason. The left-hand side of this inequality can be rewritten as

$$2 \left(\bar{G}_{ii} - \frac{\alpha\bar{u}^4}{\beta} \right) + \sum_{j \neq i} \bar{G}_{ji}.$$

The first term in the parentheses is negative because of (3.19) and the second term is a sum of negative interaction functions \bar{G}_{ji} . Hence the inequality (3.39) holds.

The remaining components in the matrix (3.38) are defined by

$$G_{\Delta k} = \frac{\bar{G}_{i,i+k} + \bar{G}_{i+k,i}}{2}. \tag{3.40}$$

We shall show that this component is independent of i . Let us start from the following integral:

$$\begin{aligned}
\int_{-x}^x \frac{\partial G_{i+k,i}}{\partial x_i} dx_i &= G_{i+k,i}(x, y) - G_{i+k,i}(-x, y) \\
&= G_{i+k,i}(x, y) - G_{i,i+k}(x, y),
\end{aligned} \tag{3.41}$$

because of (3.8) and the identity of the i th and $(i + k)$ th vortex systems. It should be pointed out that $G_{i+k,i}(-x, y)$ is equal to $G_{i,i+k}(x, y)$. On the other hand the integrand on the left-hand side of (3.41) is an even function of x , and hence one obtains

$$\int_{-x}^x \frac{\partial G_{i+k,i}}{\partial x_i} dx_i = 2 \int_0^x \frac{\partial G_{i+k,i}}{\partial x_i} dx_i = 2 (G_{i+k,i}(x, y) - G_{i+k,i}(0, y)). \quad (3.42)$$

Subtraction of (3.41) from (3.42) yields

$$G_{i+k,i}(x, y) + G_{i,i+k}(x, y) - 2G_{i+k,i}(0, y) = 0,$$

that is

$$\frac{G_{i+k,i}(x, y) + G_{i,i+k}(x, y)}{2} = G_{i+k,i}(0, y). \quad (3.43)$$

The left-hand side of the relation above is equal to $G_{\Delta k}$, and the right-hand side is a function of y , or k , only. Therefore $G_{\Delta k}$ is independent of x , or i . It is also pointed out that $G_{\Delta k}$ corresponds to an interaction function among birds flying in a straight transverse line, and that the suffix k represents a transverse distance between k birds. Hence the following relations hold:

$$G_{\Delta 1} < G_{\Delta 2} < \cdots < G_{\Delta n-1} < 0. \quad (3.44)$$

The relation between $G_{\Delta 0}$ and $G_{\Delta 1}$ can be evaluated by use of (3.19) and (3.27):

$$\begin{aligned} G_{\Delta 0} &= \bar{G}_{11} + G(n) - \frac{2\alpha\bar{u}^4}{\beta} \\ &< \bar{G}_{11} + G(2) - \frac{2\alpha\bar{u}^4}{\beta} \\ &= \bar{G}_{11} + \frac{1}{2} (\bar{G}_{11} + \bar{G}_{21} + \bar{G}_{12} + \bar{G}_{22}) - 2\frac{\alpha\bar{u}^4}{\beta} \\ &= 2 \left(\bar{G}_{11} - \frac{\alpha\bar{u}^4}{\beta} \right) + G_{\Delta 1} \\ &< G_{\Delta 1}. \end{aligned} \quad (3.45)$$

It is easy to show that the matrix \mathbf{G} is negative definite. The determinant of an n -dimensional matrix is equal to the volume of a parallelepiped in n -dimensional space, if the vertices of this parallelepiped are defined by the column vectors of this matrix (see for example Strang, 1976). All the components of all the column vectors in \mathbf{G} are negative and non-zero. Therefore the volume of the parallelepiped spanned by \mathbf{G} is positive for even n , and this volume is negative for odd n . Hence the following holds:

$$(-1)^n |\mathbf{G}| > 0,$$

which means \mathbf{G} is negative definite. Therefore one reaches the conclusion

$$\dot{H} = -\beta\bar{u}^{-3} \delta\mathbf{u}^T \mathbf{G} \delta\mathbf{u} < 0, \quad (3.46)$$

for non-zero disturbances. Because of (3.34) and (3.46), disturbances decay, and hence the formation flight is asymptotically stable.

Let us proceed to discuss the effect due to thrust fluctuation $\delta\tau_i \exp(i\Omega t)$. This acts as a forcing term in (3.21) and induces disturbances in δx_i and δu_i . The existence of a Liapunov function, having the nature (3.46), implies that all the eigenvalues of the Jacobian of the system (3.32) are negative. Let λ_i be i th eigenvalue of the Jacobian, then the effect due to the forcing is given by the convolution

$$\int_0^t \exp[\lambda_i(t - \tau)] \exp(i\Omega\tau) d\tau = -\frac{i\Omega + \lambda_i}{\Omega^2 + \lambda_i^2} \exp(i\Omega t) + \frac{i\Omega + \lambda_i}{\Omega^2 + \lambda_i^2} \exp(\lambda_i t).$$

The last term in the right-hand side of the equation above converges, as t tends to infinity. The first term, however, remains. Let δ_i be an amplitude of a disturbance in δx_i induced by thrust fluctuation. One obtains the relations

$$\begin{aligned} c_{\max} \dot{x}_i &= u_i \\ &= \bar{u} + \delta_i \cos \Omega t, \\ \dot{u}_i &= -\Omega \delta_i \sin \Omega t. \end{aligned}$$

One can rewrite these relations as

$$(u_i - \bar{u})^2 + (\dot{u}_i / \Omega)^2 = \delta_i^2. \quad (3.47)$$

This constitutes a limit cycle solution, which depicts an ellipse with its centre of foci at $(u_i, \dot{u}_i) = (\bar{u}, 0)$ in the phase plane. In this case formation flight exists in a time-averaged sense, and each bird flies to and fro around an average position in the formation. If all the birds flap their wings synchronously, the configuration of birds is unchanged from that of the steady-state solution.

4. Numerical results and discussion

This section presents specific configurations of formation flight. Sample calculations are confined to the cases of birds having the same parameters and flying at the same transverse interval, because the existence and stability of formation flight is proved for these cases only in the previous section.

4.1 Assumptions on numerical examples

To carry out numerical calculation, one needs to specify a bird and its parameters, α , β , $\bar{\tau}$. This study uses the European cormorant *Phalacrocorax carbo*, which is known to fly in a formation. Basic data can be found in Tennekes (1996) and Azuma (1992):

$$\begin{aligned} mg &= 21.0 \text{ [N]}, \\ S &= 0.250 \text{ [m}^2\text{]}, \\ \text{full span} &= 1.60 \text{ [m]}, \\ \text{cruising speed} &= 14.9 \text{ [m s}^{-1}\text{]}, \\ C_{D0} &= 0.0500. \end{aligned}$$

Physical data are as follows:

$$\begin{aligned}\rho &= 1.25 \text{ [kg m}^{-3}\text{]}, \\ g &= 9.80 \text{ [m s}^{-2}\text{]}.\end{aligned}$$

Replacing the $\bar{\tau} - \delta\tau_i$ term with $\bar{\tau}$ in (3.11) and using the data above, one obtains the parameters

$$\begin{aligned}\alpha &= 0.00365 \text{ [m}^{-1}\text{]}, \\ \beta &= 40.9 \text{ [m}^3 \text{s}^{-4}\text{]}, \\ \bar{\tau} &= 0.994 \text{ [m s}^{-2}\text{]}.\end{aligned}$$

4.2 Method of solution

We want to solve $n - 1$ equations (3.24) in terms of n bird locations. The discrepancy between the numbers of equations and unknowns will be resolved by taking relative locations as unknowns. Furthermore, we can reduce the number of unknowns down to $[(n - 1)/2]$ by noting the symmetry about the streamwise centre line of a formation. We assign the number one to birds in the flock centre and count outward in the positive y -direction, and use these numbers as suffixes. Let us introduce the unknown vector defined by

$$\mathbf{x} = (x_2, x_3, \dots, x_m)^T. \quad (4.1)$$

where $\{x_i\}$ denotes the x -component of distance between the centre of the bound vortex of the bird in the centre of the flock and that of the i th bird; the number m is given by

$$m = \left[\frac{n-1}{2} \right].$$

The basic equations can be rewritten in a vector form:

$$\mathbf{f}(\mathbf{x}) = \mathbf{0}, \quad (4.2)$$

where

$$\mathbf{f}(\mathbf{x}) = (f_1, f_2, \dots, f_{m-1})^T, \quad (4.3)$$

and

$$f_i = \sum_{j=1}^m \left[\left\{ \bar{G}_{ji} + \bar{G}_{ji}^* \right\} - \left\{ \bar{G}_{ji+1} + \bar{G}_{ji+1}^* \right\} \right];$$

\bar{G}_{ji}^* is an interaction function having x_{ji} and $y_{ji} + 2y_i$ as indices; y_i is the y -component of the i th bird's position vector.

We shall solve (4.2) in terms of (4.1) by use of Newton–Raphson method. Let $\mathbf{x}^{(n)}$ be the n th approximation, and the iteration process shall be given by

$$\mathbf{x}^{(n)} = \mathbf{x}^{(n-1)} - \left(\frac{\partial \mathbf{f}}{\partial \mathbf{x}} \right)_{\mathbf{x}=\mathbf{x}^{(n-1)}}^{-1} \cdot \mathbf{f}(\mathbf{x}^{(n-1)}). \quad (4.4)$$

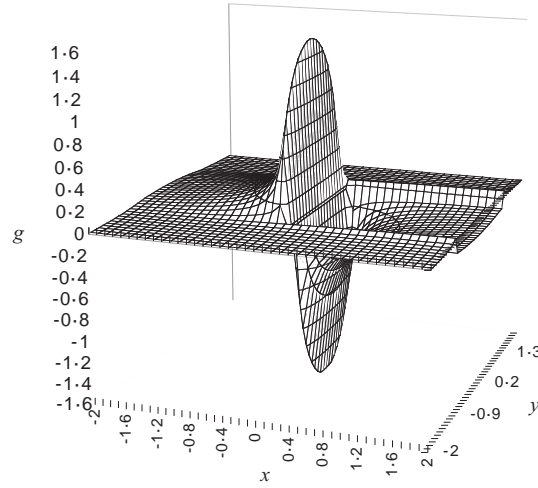


FIG. 5. Non-dimensional induced-velocity distribution around an elliptic lifting-line system in $z = 0$ plane. The distribution of g in terms of x and y is given by (3.5).

To evaluate the convergence of this iterative process, we adopt the following threshold upon a relative error:

$$\frac{|\mathbf{x}^{(n)} - \mathbf{x}^{(n-1)}|}{|\mathbf{x}^{(n)}|} < 10^{-7}.$$

In this process one needs to calculate the interaction functions (3.4), which consists of the calculation of induced velocity (3.5) and weighted integration of it.

As summarized by Abramowitz & Stegun (1972), the process of the arithmetic-geometric mean, starting from modulus and co-modulus, converges to the complete elliptic integrals up to 16 significant digits within five or six iterations.

In Fig. 5, the induced velocity distribution around an elliptic lifting-line system is depicted by this numerical evaluation of the complete elliptic integrals. There are singularities at the edges of a wing and its wake. This is due to the first term in the right-hand side of (3.5) and not related to the complete elliptic integrals. It is necessary to take care of these singularities in order to evaluate the integral (3.3). Judging from the weighting function $\sqrt{1 - \eta^2}$ in (3.3), the best choice of numerical integration is the Gaussian quadrature based on the Tchebychev polynomials of the second kind (Abramowitz & Stegun, 1972):

$$\int_{-1}^1 \sqrt{1 - \eta^2} g(x_{ji}, Y_{ji}) d\eta \approx \sum_{k=1}^N \frac{\pi \sin^2 \theta_k}{N + 1} g(x_{ji}, Y_{j_{i_k}}), \quad (4.5)$$

where N is the number of pivotal points;

$$\theta_k = \frac{k}{N+1}\pi;$$

and

$$Y_{ji_k} = \cos \theta_k + |y_{ji}|.$$

In the close vicinity of a wing tip, 0.1 times semi-span clearance, a series of test calculation about the first term in (3.5) was carried out. It was shown that numerical results converged up to 15 significant digits with 33 pivotal points. Therefore this study adopted a 33-point Gaussian quadrature. This is the most accurate result ever obtained.

4.3 Annotation of the results

This section discusses configurations of birds in a flock, that corresponds to the steady-state solution to (2.8), and their effects on energy-saving flight.

Figure 6 shows how the transverse interval between wing tips affects configurations. The number of birds is fixed at ten in these numerical calculations. The larger the intervals become, the flatter the configurations. One bird's location in a flock becomes less important as the transverse distances between birds become larger. Flight in a formation carries few advantages, if transverse intervals are greater than several semi-spans.

Figure 7 shows how the number of birds affects configurations. These numerical results are obtained for an interval fixed at 0.1 times semi-span.

In the case of two birds the discussion in Section 3.3 and (3.24) reveals that a possible solution corresponds to a side-by-side configuration. I did not include this trivial case in Fig. 7.

As shown in Figs 6 and 7, the stable solutions assume parabola-like U configurations for any numbers of birds. A twofold mechanics makes such a configuration: (1) as described by the induced velocity distribution function g in Fig. 5, favourable upwash induced by flock members increases in the downstream direction and decreases in the transverse direction; (2) birds in-between their flock members can gain upwash from both sides, while birds at edges of the flock obtain upwash from one side only. Therefore birds in-between are pushed forward, and edge birds stay behind their flock members. Thus a U configuration emerges.

Flying within the U configuration, every bird has the same amount of induced drag in the flock. Flying ahead is less advantageous to reduce drag, while flying behind within this configuration saves more energy.

As Fig. 8 shows, birds do fly in U formation. But more often they fly in wedge-like V formations. In such formations leading birds indeed fly harder than trailing birds. It should, however, be emphasized that even a leading bird can fly more easily in a formation than it flies alone, because flying in other birds' upwash always reduces drag. This is confirmed by the field observations of V formation (Weimerskirch *et al.*, 2001).

Field observation also raises the question of why a real configuration is frequently rearranged to a larger extent. One possible reason is due to transient disturbances like gust. Another possibility is attributed to the living nature of birds' formations. Reynolds (1987)

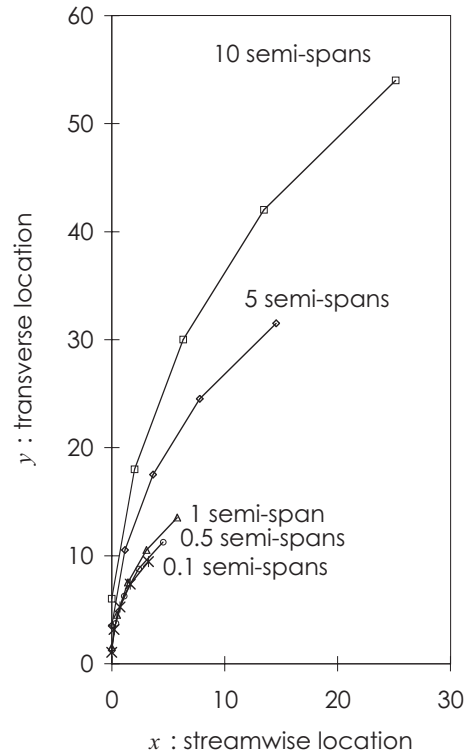


FIG. 6. Configurations of 10 birds with various transverse intervals. The coordinate system x and y are nondimensionalized by use of the root chord c_{\max} and the semi-span $s/2$, respectively. The transverse intervals are given adjacent to the corresponding configurations.

studied the flocking mechanism. His heuristic model, called *boid*, does not incorporate any physics, but simulates flocking features as follows:

- (1) Collision avoidance: avoid collisions with nearby flock members;
- (2) Velocity matching: attempt to match velocity with nearby flock members;
- (3) Flock centring: attempt to stay close to nearby flock members.

His *boids* do not fly in a formation like the present results but they fly like a flock of starlings. In reality birds fly in a formation because of physical as well as biological reasons and hence formations observed in the fields are not always inverted U.

Let us discuss energy-saving effects. Figure 9 shows variation of cruising velocities in formations with various intervals and numbers of birds. The cruising speed in solo flight is 14.9 m s^{-1} , while cruising speeds can be as fast as 16 m s^{-1} . The distance between birds is the most important of aerodynamic interactions, so the interval between birds becomes the primary factor to enhance terminal velocities: the closer birds fly together, the more easily they can fly. The number of birds is the secondary factor to make flight effective. The effect of remote birds diminishes as the number of birds increases.

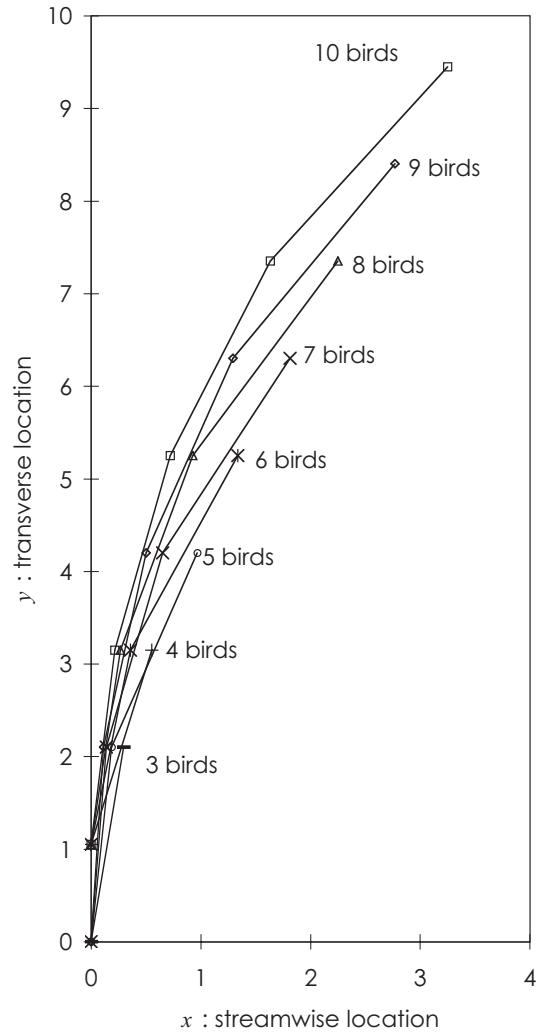




FIG. 8. Migrant cranes flying in the U configuration (Schlichting, 1942).

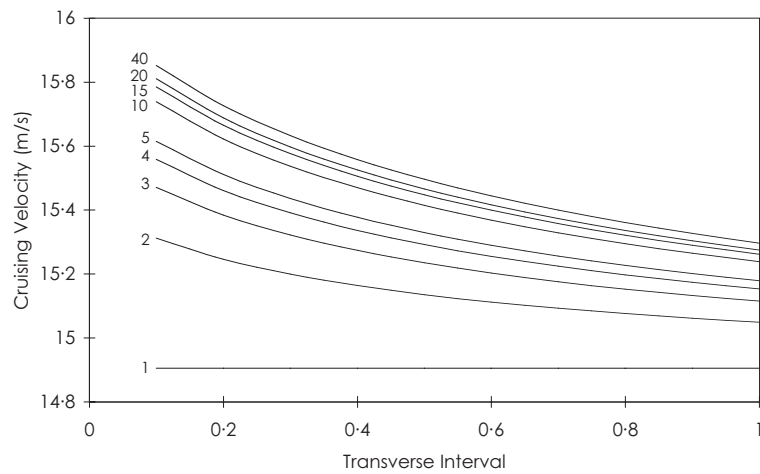


FIG. 9. Relations between cruising velocity, transverse interval, and the number of birds. The number of birds is given adjacent to lines. The abscissa, the transverse interval between wing tips, is nondimensionalized by $s/2$.

possible, drag can even be halved. Earlier studies (Wieselsberger, 1914; Schlichting, 1942; Hummel, 1973, 1978, 1983, 1995, 1996; Filippone, 1996) emphasized the effect on drag reduction, and the present prediction agrees qualitatively with their results. A small amount of quantitative discrepancy is attributed to the difference in models, i.e. a constant strength vortex or elliptic vorticity distributions.

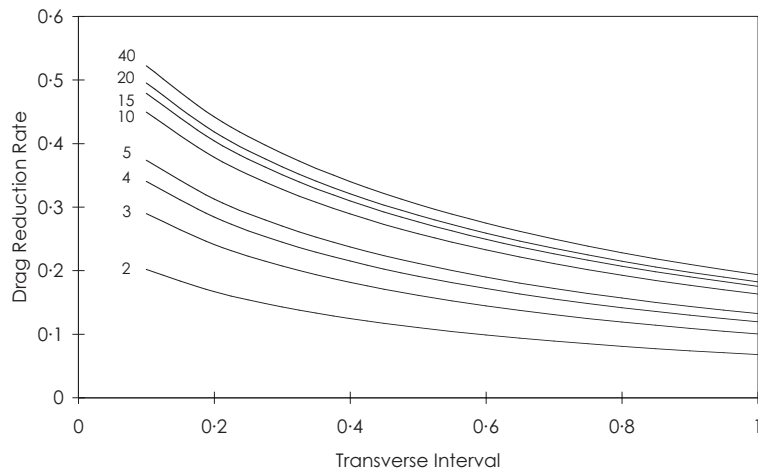


FIG. 10. Relations between drag reduction rate, transverse interval, and the number of birds. Drag reduction rate is given by (4.6). The number of birds is given adjacent to lines. The abscissa, the transverse interval between wing tips, is nondimensionalized by $s/2$.

5. Conclusions

This study has analysed formation flight as the complex dynamical system (2.8), and has revealed the following facts:

- (1) Formation flight is not always feasible. There exists a necessary condition (3.20). If this necessary condition is fulfilled, then the cruising state behaves as a global attractor.
- (2) Formation flight among physically identical birds does exist and is stable in a Liapunov sense. If the thrust is constant, formation flight (3.22) is asymptotically stable. If thrust fluctuates periodically, there exists a limit cycle solution (3.47) moving around a formation-flight solution of constant thrust. The dynamical system (2.8) does not exhibit chaotic behaviour.
- (3) The presented method of solution (4.4) is semi-analytic, quickly converging and very accurate. Numerical calculations reach stable solutions, which closely resemble the solutions given by former studies. Parabola-like U configurations are found for the steady-state solutions to (2.8). In these configurations the same amount of drag acts on every bird. These configurations emerge in a self-organizing manner.
- (4) In a formation every flock member has some advantage of reducing its induced drag. Even in a V formation a leading bird suffers less drag than flying alone.

The study affords primary information about the dynamics of formation flight. The result is, however, still confined to the realm of idealization, for the theoretical basis relies on steady lifting-line theory. There remain challenges to be studied in this vast field: the formation dynamics of birds with different parameters, motion with more degrees of freedom, and so on.

Acknowledgements

Final development of the theory was done in the Department of Applied Mathematics and Theoretical Physics, University of Cambridge during my study leave from Kanagawa University. I am very grateful for the hospitality and generosity of these institutions and their people, in particular my host Professor T. J. Pedley as well as Professors M. Kitaoka and K. Narita, the former and the present heads of the department in Japan. Without this support I could not have completed the study in the present form.

REFERENCES

- ABRAMOWITZ, M. & STEGUN, I. A. (1972) *Handbook of Mathematical Functions*, Reprinted edition, New York: Dover.
- AZUMA, A. (1992) *The Biokinetics of Flying and Swimming*, First edition, Tokyo: Springer, 114.
- BEUKENBERG M. & HUMMEL, D. (1986) Flugversuche zur messung der leistungersparnis im verbandsflug. *Jahrb. Deutsch. Ges. Luft-Raumfahrt*, **1**, 133–145.
- BRYSON, A. E. JR. & HO, Y.-C. (1975) *Applied Optimal Control*, Revised edition, Washington, DC: Hemisphere, 108.
- FILIPPONE, A. (1996) Heuristic optimization applied to an intrinsically difficult problem: birds formation flight. *AIAA Paper*, **96-0515**, 1–12.
- HUMMEL, D. (1973) Die leistungersparnis beim verbandsflug. *J. Ornithol.*, **144**, 259–282.
- HUMMEL, D. (1978) Die leistungersparnis in flugformationen von Vögeln mit Unterschieden in Größe, Form und Gewicht. *J. Ornithol.*, **149**, 52–73.
- HUMMEL, D. (1983) Aerodynamic aspects of formation flight in birds. *J. Theor. Biol.*, **104**, 321–347.
- HUMMEL, D. (1995) Formation flight as an energy-saving mechanism. *Isr. J. Zool.*, **41**, 261–278.
- HUMMEL, D. (1996) The use of aircraft wakes to achieve power reductions in formation flight. *AGARD-CP-584*, 36–1–13.
- HUMMEL, D. & BEUKENBERG, M. (1989) Aerodynamische interferenzeffekte beim formationsflug von Vögeln. *J. Ornithol.*, **130**, 15–24.
- HUMMEL, D. & BOCK, K. W. (1981) Leistungersparnis durch formationsflug. *Z. Flugwiss. Weltraumforsch.*, **5**, 148–162.
- LIGHTHILL, J. (1989) *An Informal Introduction to Theoretical Fluid Mechanics*, Revised edition, Oxford: Oxford University Press, 200–228.
- LISSAMAN, P. B. S. & SHOLLENBERGER, C. A. (1970) Formation flight of birds. *Science*, **168**, 1003–1005.
- MILNE-THOMSON, L. M. (1973) *Theoretical Aerodynamics*, New York: Dover.
- OHANIAN, H. (1998) Question #71. Birds and bombers—why the V-formation. *Am. J. Phys.*, **66**, 275.
- PHILLIPS, J. D. (1985) Downwash in the plane of symmetry of an elliptically loaded wing. *NASA Tech. Paper*, **2414**, 1–21.
- RAYNER, J. M. V. (2001) Fat and formation in flight. *Nature*, **413**, 685–686.
- REYNOLDS, C. W. (1987) Flocks, herds, and schools: a distributed behavioral model. *Comp. Graphics*, **21**, 25–34.
- SAFFMAN, P. G. (1992) *Vortex Dynamics*, First edition, Cambridge: Cambridge University Press, 46.
- SCHLICHTING, H. (1942) Leistungersparnis in verbandsflug. *Bericht Aerodyn. Inst. T. H. Braunschweig*, **42/6**, English translation: *TMB Translation* 1951 **239**, US Navy.
- SCHLICHTING, H. (1944) Verbandsflug mit hohenstaffelung. *Bericht Aerodyn. Inst. T. H. Braunschweig*, **44/7**, English translation: *TMB Translation* 1950 **240**, US Navy.
- STRANG, G. (1976) *Linear Algebra and its Applications*, New York: Academic, 147.

- SUGIMOTO, T. (2002) Induced velocity in the plane of an elliptically loaded lifting line. *AIAA J.*, **40**, 1233–1236.
- TENNEKES, H. (1996) *The Simple Science of Flight*, English edition, Cambridge, MA: MIT Press, 131.
- WEIMERSKIRCH, H., MARTIN, J., CLERQUIN, Y., ALEXANDRE, P. & JIRASKOVA, S. (2001) Energy saving in flight formation. *Nature*, **413**, 697–698.
- WIESELSBERGER, C. (1914) Beitrag zur erklärung des winkelfluges einerer zugvogel. *Z. Flugtechnik & Motorluftschiffahrt*, **5**, 225–229.
- WILMOTT, P. (1988) Unsteady lifting-line theory by the method of matched asymptotic expansions. *J. Fluid Mech.*, **186**, 303–320.

Appendix. Long-distance horizontal flight in minimum time

This appendix explains why constant thrust is assumed in this study on the basis of optimum control theory: e.g. Bryson & Ho (1975).

The problem, how to control the thrust τ_i to travel for a given distance in minimum time, is mathematically formulated as follows. Suppose t_f denotes travelling time, then:

$$\text{Minimize } t_f = \int_0^{t_f} dt$$

subject to the state equation (2.8), the integral constraint on a distance

$$\int_0^{t_f} u_i dt = D,$$

and the lower and upper bounds on the control variable

$$0 \leq \tau_i \leq \tau_{\max}.$$

In the expression above D and τ_{\max} denote the given distance and the maximum thrust, respectively.

Introducing Lagrange multipliers λ_1 and λ_2 , one can extend the objective as follows:

$$\int_0^{t_f} dt + \int_0^{t_f} \lambda_1 \left\{ \dot{u}_i - \alpha_i u_i^2 - \sum_{j=1}^n \beta_j G_{ji} u_i^{-1} u_j^{-1} + \tau_i \right\} dt + \lambda_2 \left\{ \int_0^{t_f} u_i dt - D \right\}.$$

In other words, the Hamiltonian of the problem, H , assumes the form

$$H = 1 + \lambda_1 \left\{ \dot{u}_i - \alpha_i u_i^2 - \sum_{j=1}^n \beta_j G_{ji} u_i^{-1} u_j^{-1} + \tau_i \right\} + \lambda_2 u_i.$$

This is a linear function of τ_i , and hence has extremal at the boundary values of the control variable:

$$\tau_i = \begin{cases} \tau_{\max} & \text{if } \lambda_1 > 0, \\ 0 & \text{if } \lambda_1 < 0. \end{cases}$$

The positive λ_1 corresponds to the acceleration phase, while the negative λ_1 corresponds to the deceleration phase. Therefore the constant thrust is practically meaningful in an optimum control sense.